Electronic Supplementary Information (ESI)

Simultaneous analyte indicator binding assay (SBA) for the monitoring of reversible host-guest complexation kinetics

Zsombor Miskolczy,[a] Mónika Megyesi,[a] Stephan Sinn,[b] Frank Biedermann,[*b] and László Biczók[*a]

[a]*Research Centre for Natural Sciences, Institute of Materials and Environmental Chemistry, Eötvös Loránd Research Network (ELKH), P.O. Box 286, 1519 Budapest, Hungary*

[b]*Institute of Nanotechnology (INT), Karlsruhe Institute of Technology (KIT), Hermann-von-Helmholtz-Platz 1, 76344 Eggenstein-Leopoldshafen, Germany*

[*] Corresponding author. E-mail: biczok.laszlo@ttk.hu
[*] Corresponding author. E-mail: frank.biedermann@kit.edu
Supporting Information for this article is available on the WWW under http://dx.doi.org

MATERIALS AND METHODS

Berberine and palmatine (Sigma-Aldrich) was chromatographed on silica gel (Merck) column eluting with ethanol. Dehydrocorydaline chloride (DHC, BOC Sciences), (+)-fenchone ((1*S*)-1,3,3-trimethylbicyclo[2.2.1]heptan-2-one) (Sigma-Aldrich), norcamphor (Acros Organics), 2,2,6-trimethylcyclohexanone (Alfa Aesar), cyclohexanone (Sigma-Aldrich), 2-adamantanone (TCI), 5-chloro-2-adamantone (TCI), 5-bromo-2-adamantone (TCI), *trans*-4-[4-(dimethylamino)styryl]-1-methylpyridinium iodide (DSMI, Sigma Aldrich), cadaverine dihydrochloride (CAD, Sigma Aldrich), 4-methylbenzylamine (4-MBA, Acros Organics), and cucurbit[6]uril (CB6, Strem Chemicals) were used as received. Iodide salt of 6-methoxy-1-methylquinolinium was synthesized as reported previously.[1] High-purity CB7 was kindly provided by Dr. Anthony I. Day (University of New South Wales, Canberra, Australia). Experiments were performed in water freshly distilled twice from dilute $KMnO_4$ solution.

The UV-visible absorption spectra were measured on an Agilent Technologies Cary60 spectrophotometer. Corrected fluorescence spectra were recorded on a Jobin-Yvon Fluoromax-P spectrofluorometer. Stopped-flow measurements were carried out with the same instrument using an Applied Photophysics RX2000 rapid mixing accessory and a pneumatic drive. The temperature of the samples was controlled with a Julabo F25-ED thermostat. The results of spectrophotometric and fluorescence titrations as well as stopped-flow measurements were analysed with homemade programs written in MATLAB 7.9. The ode45 function of the MATLAB optimization toolbox, which is based on an explicit Runge-Kutta (4,5) formula,[2] was used to solve systems of differential equations. Isothermal calorimetric titrations were performed with a VP-ITC (MicroCal) instrument at 298 K. Guest solution was injected stepwise into CB7 solutions, while stirring at 300 rpm. The dilution heat, which was obtained by adding guest solution into water under the same conditions as in

the titration of CB7, was subtracted from the integrated heat released per injection, and the result was divided by the mole number of injectant. Data were analysed using the one-site binding model and Microcal ORIGIN software. The first data point was always removed. The measurements were repeated at least three times.

For the inclusion studies with CB6, fluorescence kinetic traces were acquired by stopped-flow experiments on a Jasco FP-8300 fluorescence spectrometer equipped with a thermostated (298 K) SFA-20 stopped-flow accessory from TgK Scientific Limited driven by pneumatic drives. Stock solutions of CB6, DSMI, 4-MBA and CAD were freshly prepared in Millipore H_2O with an addition of a few drops of hydrochloric acid to 4-MBA solution to ensure pH = 7.

SIMULTANEOUS ANALYTE INDICATOR BINDING ASSAY

System of differential equations describing the binding kinetics

$$H + D + G \rightleftharpoons HD + HG \quad \text{(S1)}$$

$$H + D \underset{k_{out}^{HD}}{\overset{k_{in}^{HD}}{\rightleftharpoons}} HD \quad \text{(S2)}$$

$$H + G \underset{k_{out}^{HG}}{\overset{k_{in}^{HG}}{\rightleftharpoons}} HG \quad \text{(S3)}$$

$$\frac{d[HD]}{dt} = k_{in}^{HD}\,[H][D] - k_{out}^{HD}[HD] \quad \text{(S4)}$$

$$\frac{d[D]}{dt} = -k_{in}^{HD}\,[H][D] + k_{out}^{HD}[HD] \quad \text{(S5)}$$

$$\frac{d[HG]}{dt} = k_{in}^{HG}\,[H][G] - k_{out}^{HG}[\mathrm{HG}] \quad \text{(S6)}$$

$$\frac{d[G]}{dt} = -k_{in}^{HG}\,[H][G] + k_{out}^{HG}[\mathrm{HG}] \quad \text{(S7)}$$

$$\frac{d[H]}{dt} = -k_{in}^{HD}\,[H][D] + k_{out}^{HD}[HD] - k_{in}^{HG}\,[H][G] + k_{out}^{HG}[\mathrm{HG}] \quad \text{(S8)}$$

$$I(t) = \phi^{HD}[HD] + \phi^{D}[D] \quad \text{(S9)}$$

[H], [D], [G] – host, dye, guest concentration at time *t*

[HD], [HG] – concentration of host–dye and host–guest complexes at time *t*

I(t) – fluorescence intensity at time *t*

ϕ^{HD} – constant proportional to the fluorescence efficiency of host–dye complex at the monitoring wavelength

ϕ^{D} – constant proportional to the fluorescence efficiency of free dye at the monitoring wavelength

Evaluation of the rate constants

Stopped-flow experiments were performed monitoring the fluorescence intensity change in real time. The fluorescence intensity of the completely complexed (I_T^{HD}) and free (I_T^D) indicator dye was recorded. The kinetic traces measured at various nonfluorescent guest concentrations at the same experimental conditions ($I(t)$) were normalized using the following relationship: $I(t)_{norm} = [I(t) - I_T^D]/[I_T^{HD} - I^D]$. The system of differential equations describing the binding kinetics (*vide supra*) was solved numerically by the ode45 function of the MATLAB optimization toolbox, which is based on an explicit Runge-Kutta (4,5) formula[2]. The rate constants of the reversible confinement of the indicator (k_{in}^{HD} and k_{out}^{HD}) were fixed at the value taken from independent measurements. The rate constants of guest entry and exit (k_{in}^{HG} and k_{out}^{HG}) as well as a fluorescence intensity related fitting parameter were calculated by nonlinear least-squares regression.

The determination of the equilibrium constant for HG formation (K_{HG}) is not necessary before performing *kin*SBA experiment. The indicator dye and the initial concentrations of the components ($[D]_0$, $[G]_0$, and $[H]_0$) can be varied to obtain kinetic traces similar to those displayed in Fig. 4A or 4B. Although K_{HG} is not used in the nonlinear least-squares fit of the recorded signals, the estimation of its value helps to find the optimal initial concentrations faster. CB7 concentration of 0.25 μM is generally a good choice if $K_{HG} \geq 10^4$ M^{-1}. In the case of lower K_{HG}, larger CB7 concentration can be employed. The use of dilute host solution reduces the risk of the undesirable interference of ternary complexation. The selected indicator dye should have high fluorescence quantum yield change upon complexation and the equilibrium constant of its binding should differ preferably by less than 3 orders of magnitude from K_{HG}. The initial D and G concentrations ($[D]_0$ and $[G]_0$) should be adjusted to produce enough HD and HG in equilibrium. The accuracy of the calculated rate constants is improved if they are derived as a mean of the results of several experiments performed at various $[G]_0$ holding $[D]_0$ constant.

SIMULATED SIGNALS

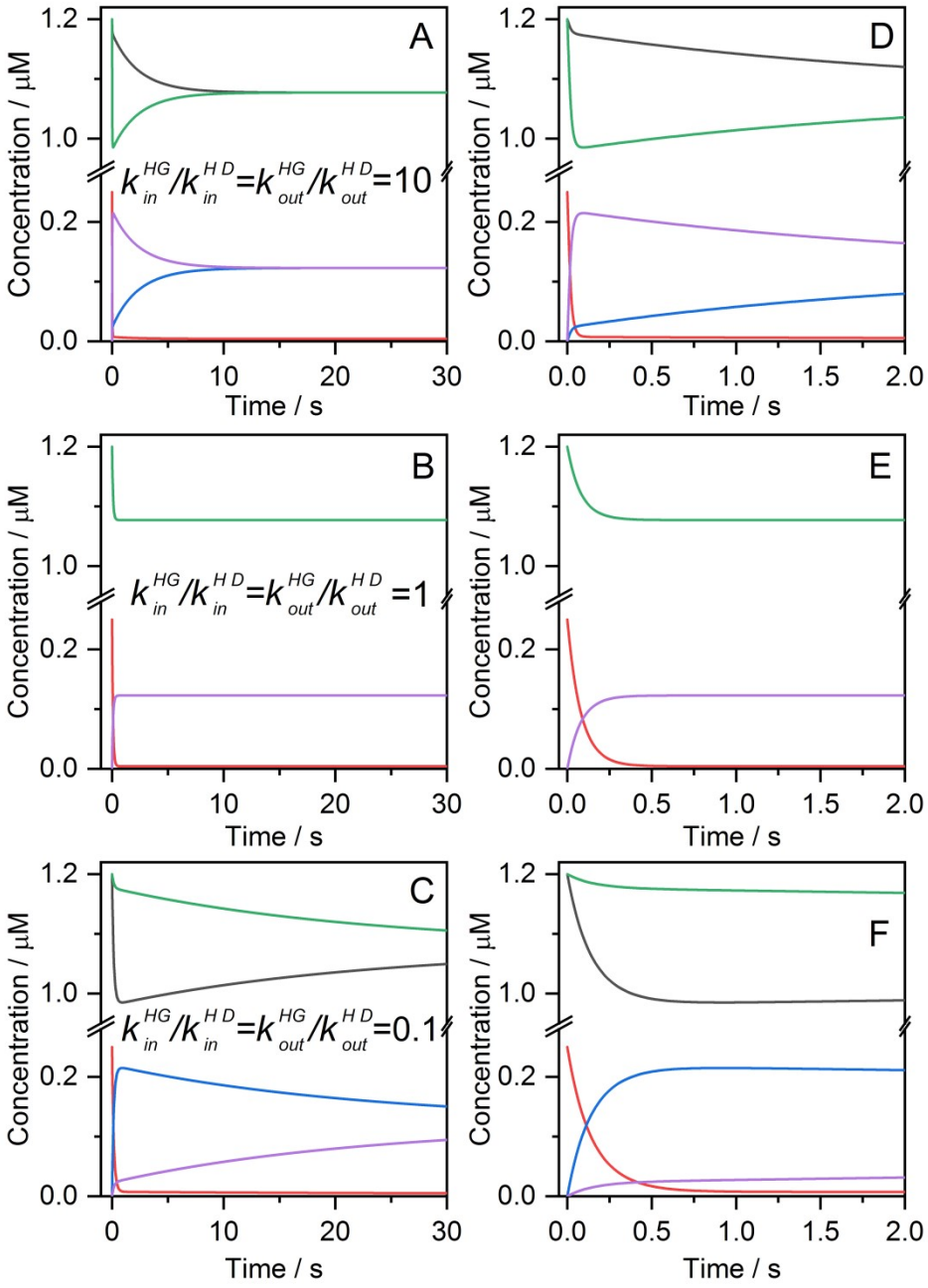

Figure S1 Simulated changes of D (black), G (green), H (red), HD (blue) and HG (violet) concentrations vs. time after mixing H solution with the solution of G and D. Concentrations at t = 0 s are [H] = 0.25 µM, [D] = [G] = 1.2 µM. Negligible fluorescence was assumed for the unbound indicator. The rate constants k_{in}^{HD} = 5.4×10^6 M^{-1} s^{-1} and k_{out}^{HD} = 0.20 s^{-1} were fixed and corresponded to those of palmatine binding with CB7, see also Table 1. (A)-(C) k_{in}^{HG} and k_{out}^{HG} was varied holding K^{HG} = 2.7×10^7 M^{-1} constant. (B) [D]=[G] and [HD]=[HG]; (D-F) represent the zoomed views.

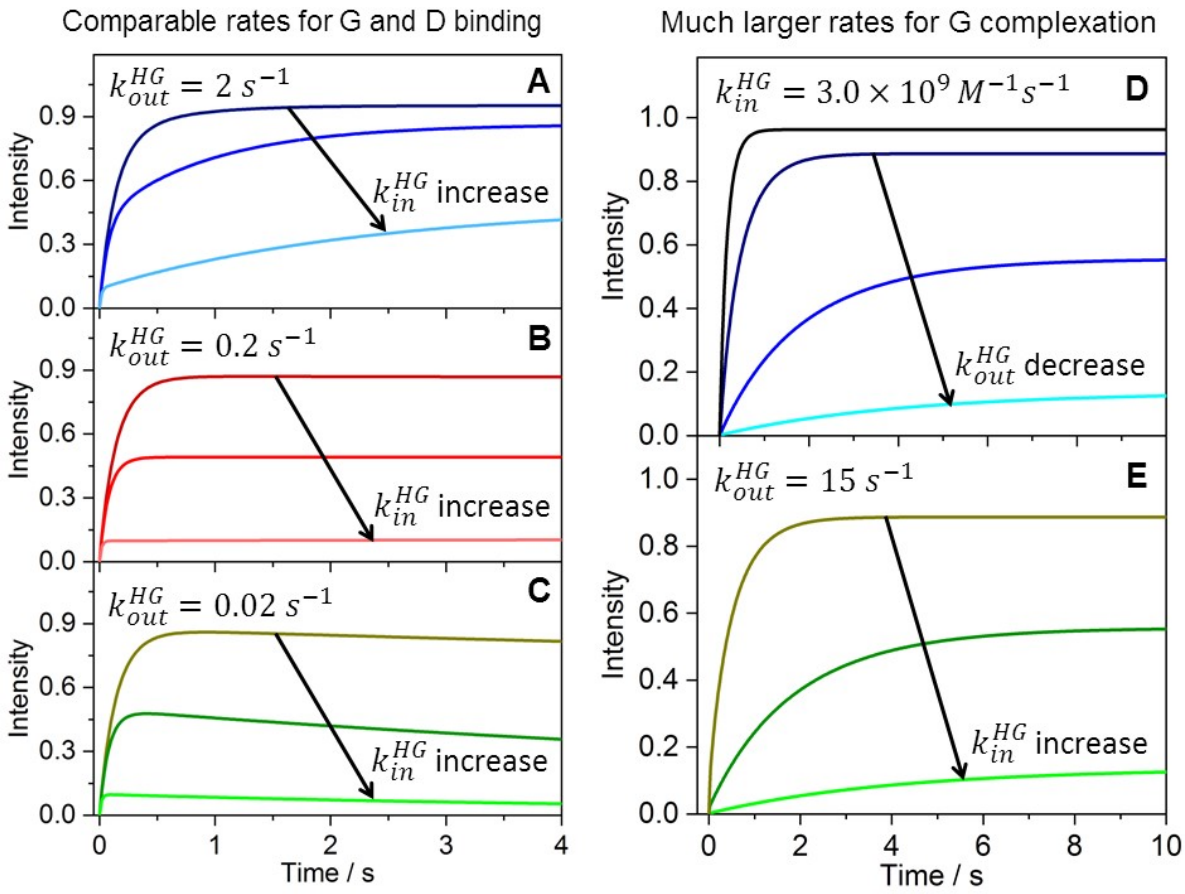

Figure S2 Simulated fluorescence intensity vs. time traces after mixing host solution with the solution of guest and indicator dye. Concentrations at t = 0 s are [host] = 0.25 μM, [indicator] = [guest] = 1.2 μM. Negligible fluorescence was assumed for the uncomplexed indicator. The rate constants k_{in}^{HD} = 5.4×10^6 M^{-1} s^{-1} and k_{out}^{HD} = 0.20 s^{-1} were fixed and corresponded to those of palmatine binding with CB7.[3] (A)–(C) k_{in}^{HG} was varied 5.4×10^5, 5.4×10^6, and 5.4×10^7 M^{-1} s^{-1} (from top to down). (D) in the absence of G and k_{out}^{HG} = 1500, 150, 15 s^{-1} (from top to down). (E) k_{in}^{HG} was changed 3.0×10^7, 3.0×10^8, and 3.0×10^9 M^{-1} s^{-1} (from top to down).

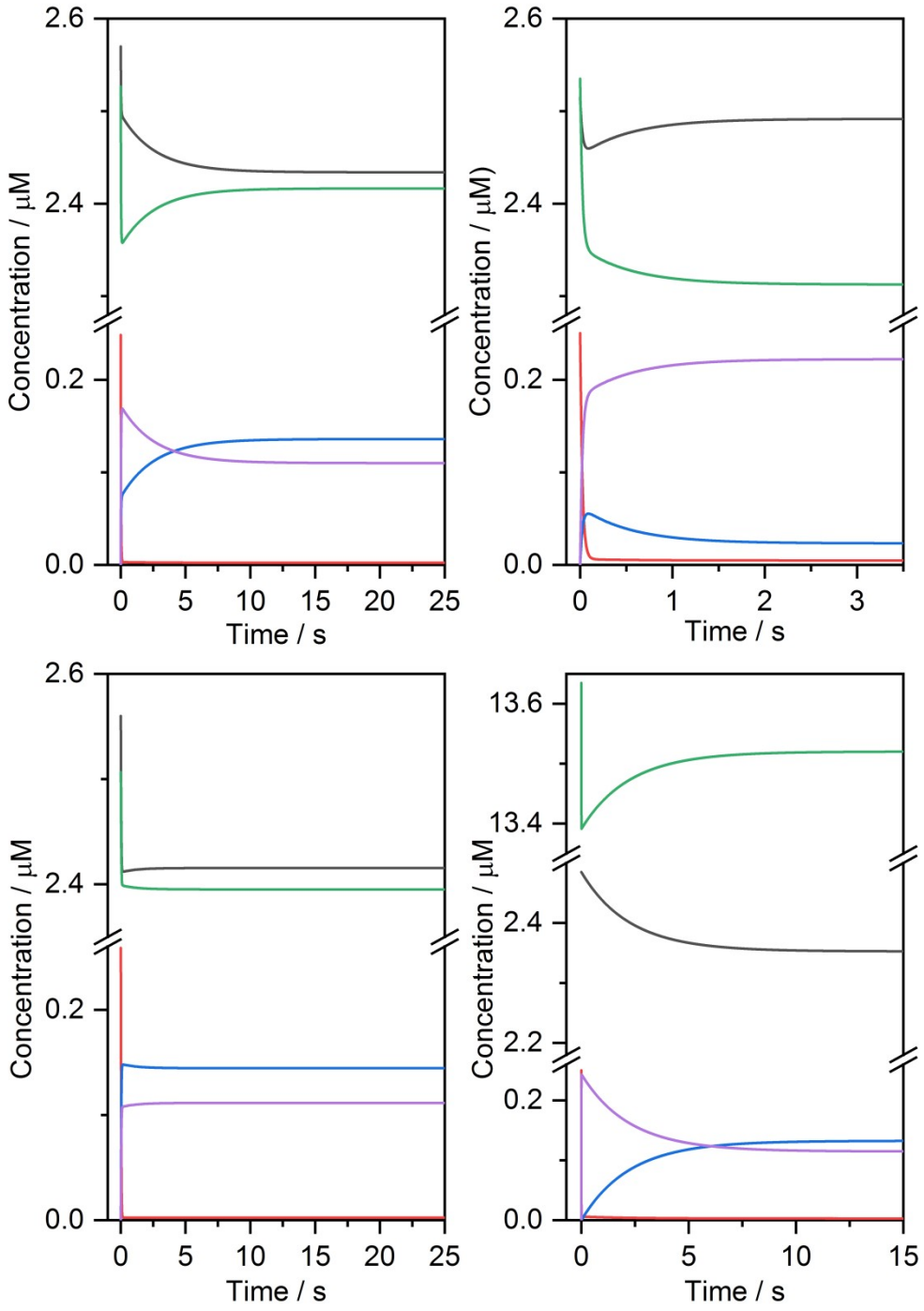

Figure S3 Changes of D (black), G (green), H (red), HD (blue) and HG (violet) concentrations vs. time corresponding to the signals displayed in Fig.4 after rapid mixing 0.25 μM CB7 solution with (A) 2.5 μM cyclohexanone and 2.5 μM palmatine solution, (B) 2.5 μM cyclohexanone and 2.5 μM DHC solution, (C) 2.5 μM cyclohexanone and 2.5 μM berberine solution, (D) 13.6 μM 6-methoxy-1-methylquinolinium and 2.5 μM palmatine solution.

RESULTS

Cyclohexanone

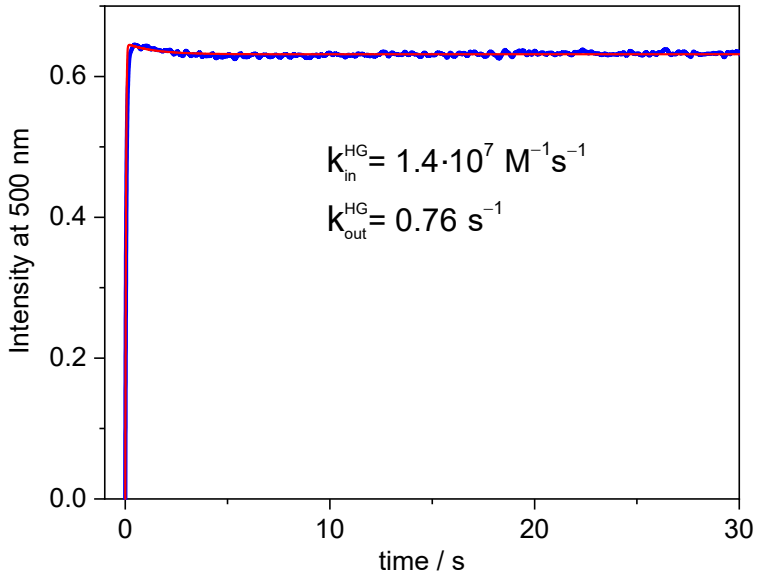

Figure S4 Fluorescence intensity change at 500 nm as a function of time in a solution of berberine and cyclohexanone after mixing with CB7 solution at 298 K. Total concentrations at t=0 s were 2.5 μM berberine, 2.5 μM cyclohexanone, and 0.25 μM CB7 Excitation occurred at 345 nm. The red line represents the result of the nonlinear least-squares fit of the numerical solution of the system of differential equations.

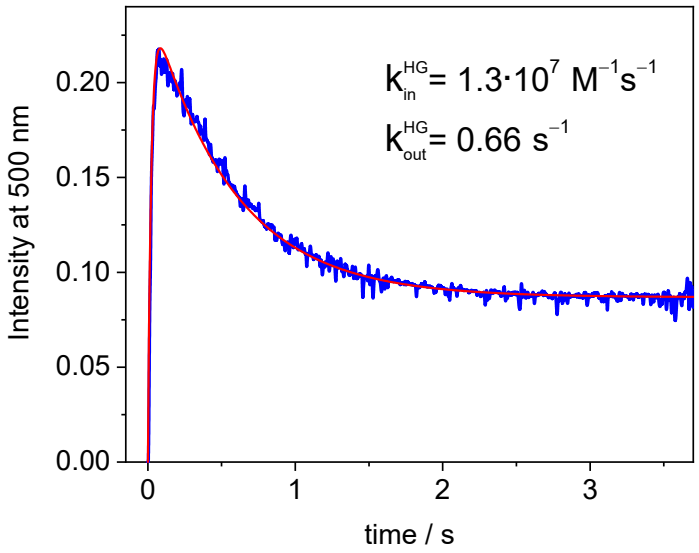

Figure S5 Fluorescence intensity change at 500 nm as a function of time in a solution of dehydrocorydaline and cyclohexanone after mixing with CB7 solution at 298 K. Total concentrations at t = 0 s were 2.5 μM dehydrocorydaline, 2.5 μM cyclohexanone, and 0.25 μM CB7 Excitation occurred at 345 nm. The red line represents the result of the nonlinear least-squares fit of the numerical solution of the system of differential equations.

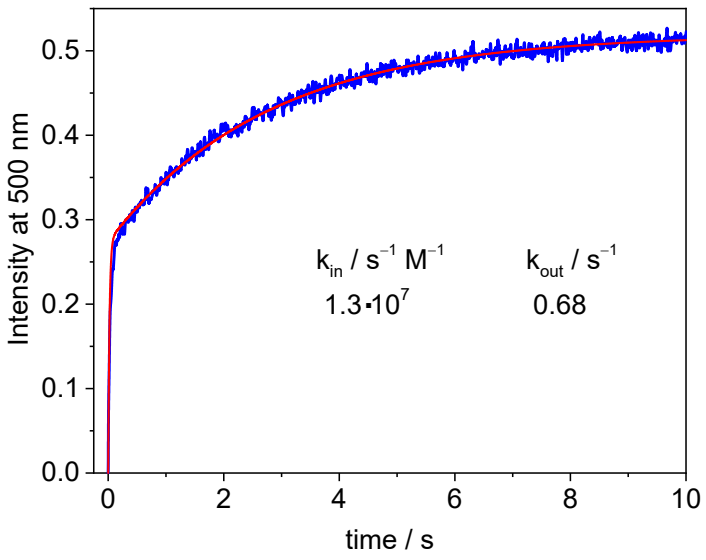

Figure S6 Fluorescence intensity change at 500 nm as a function of time in a solution of palmatine and cyclohexanone after mixing with CB7 solution at 298 K. Total concentrations at t=0 s were 2.5 μM palmatine, 2.5 μM cyclohexanone, and 0.25 μM CB7 Excitation occurred at 345 nm. The red line represents the result of the nonlinear least-squares fit of the numerical solution of the system of differential equations.

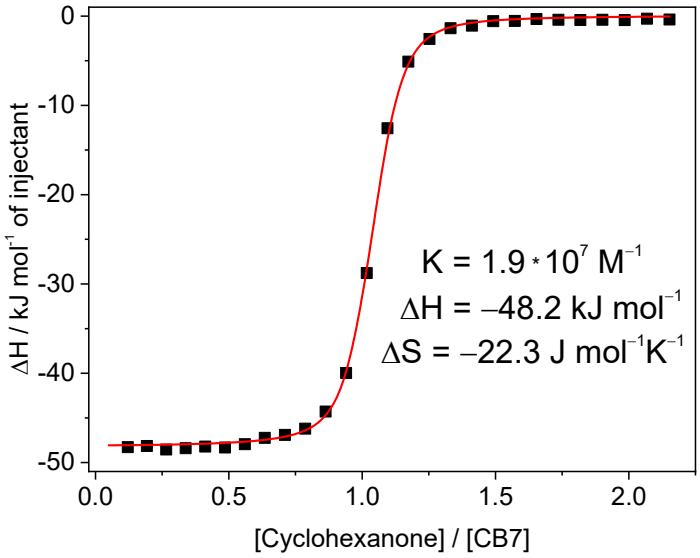

Figure S7 Integrated heat released per injection (■) for the titration of 26 μM CB7 by 268 μM cyclohexanone solution at 298 K. The line represents the best fit with a one-site binding model.

Norcamphor

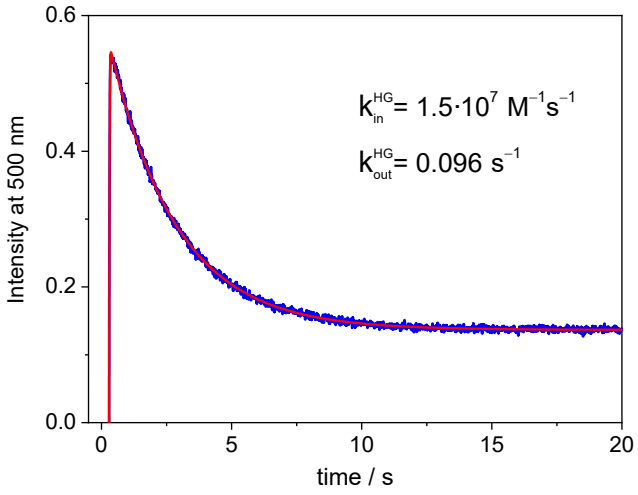

Figure S8 Fluorescence intensity change at 500 nm as a function of time in a solution of berberine and norcamphor after mixing with CB7 solution at 298 K. Total concentrations at t=0 s were 2.5 μM berberine, 2.5 μM norcamphor, and 0.25 μM CB7 Excitation occurred at 345 nm. The red line represents the result of the nonlinear least-squares fit of the numerical solution of the system of differential equations.

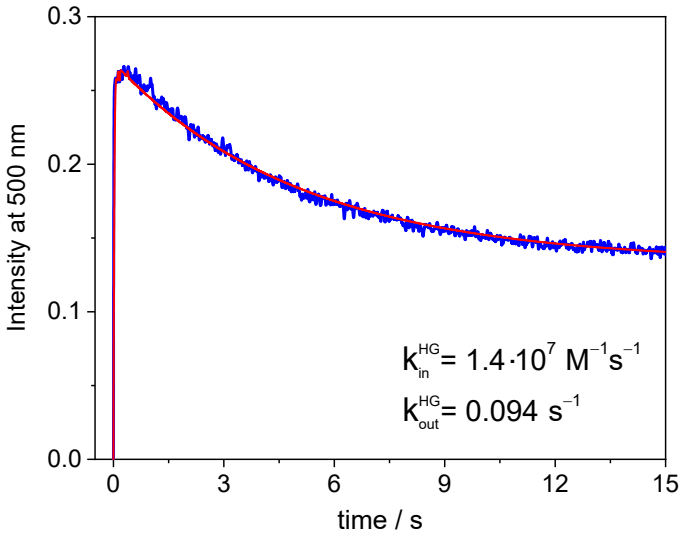

Figure S9 Fluorescence intensity change at 500 nm as a function of time in a solution of palmatine and norcamphor after mixing with CB7 solution at 298 K. Total concentrations at t=0 s were 2.6 μM palmatine, 2.6 μM norcamphor, and 0.25 μM CB7 Excitation occurred at 345 nm. The red line represents the result of the nonlinear least-squares fit of the numerical solution of the system of differential equations.

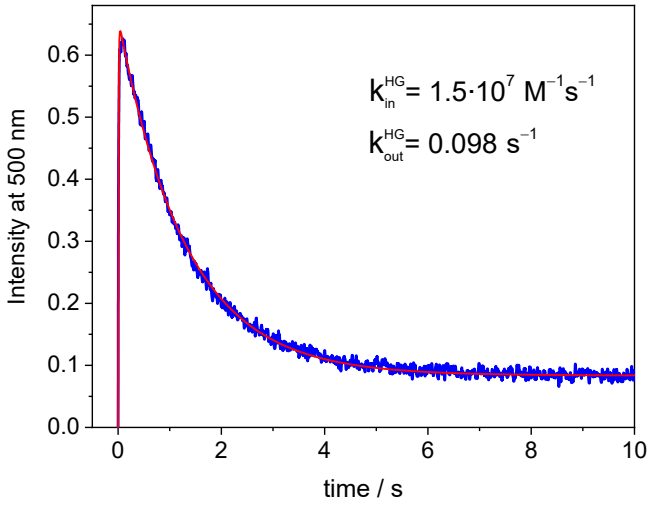

Figure S10 Fluorescence intensity change at 500 nm as a function of time in a solution of dehydrocorydaline and norcamphor after mixing with CB7 solution at 298 K. Total concentrations at t = 0 s were 20 μM dehydrocorydaline, 2.8 μM norcamphor, and 0.25 μM CB7 Excitation occurred at 345 nm. The red line represents the result of the nonlinear least-squares fit of the numerical solution of the system of differential equations.

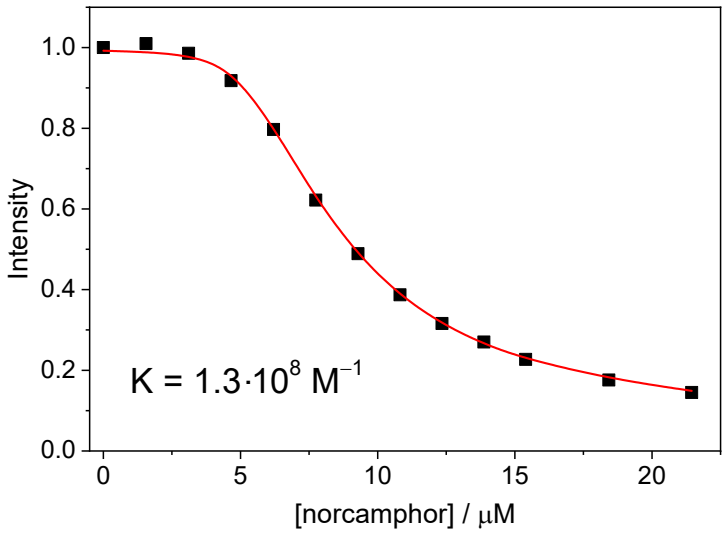

Figure S11 Fluorescence intensity at 500 nm as a function of norcamphor concentration in the solution 5.0 μM berberine and 10.6 μM CB7. Excitation was performed at 345 nm. The red line shows the result of the nonlinear least-squares fit.

2,2,6-trimethyl-cyclohexanone

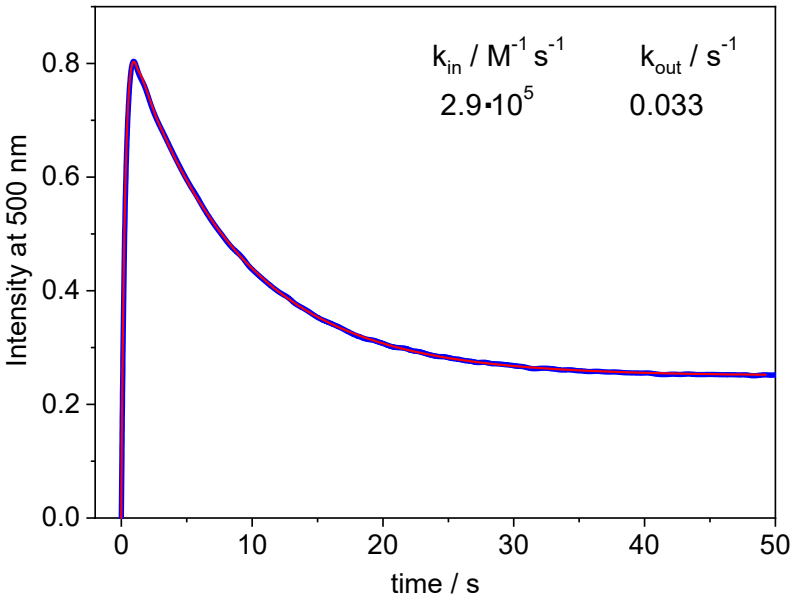

Figure S12 Fluorescence intensity change at 500 nm as a function of time in a solution of berberine and 2,2,6-trimethyl-cyclohexanone after mixing with CB7 solution at various temperatures. Total concentrations at t = 0 s were 2.5 μM berberine, 19.3 μM 2,2,6-trimethyl-cyclohexanone, and 0.25 μM CB7 Excitation occurred at 345 nm. The red lines represent the result of the nonlinear least-squares fit of the numerical solution of the system of differential equations.

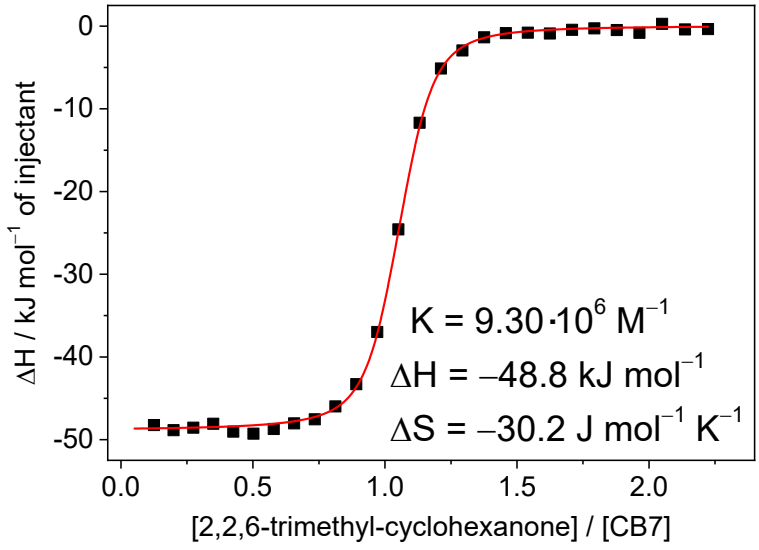

Figure S13 Integrated heat released per injection (■) for the titration of 38.8 μM CB7 by 407 μM 2,2,6-trimethyl-cyclohexanone solution at 298 K. The line represents the best fit with a one-site binding model.

(+)-fenchone

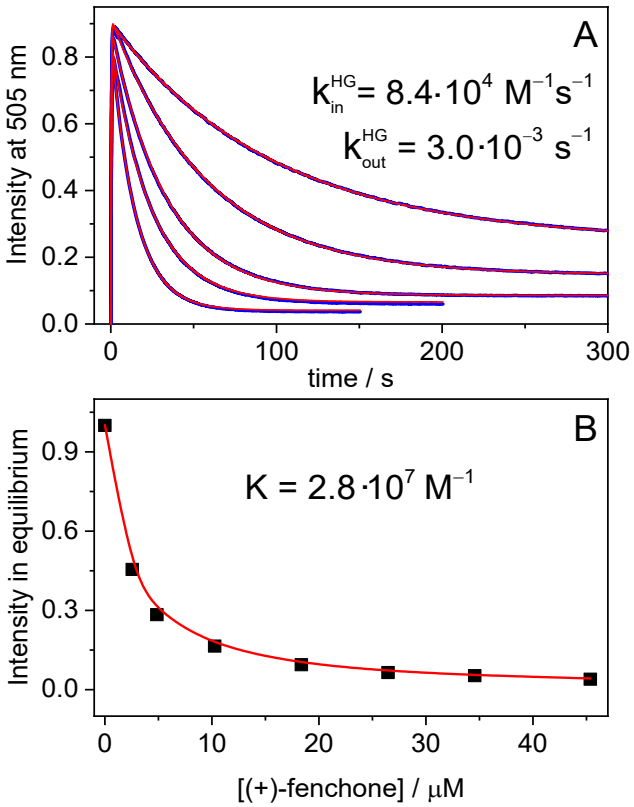

Figure S14 (A) Fluorescence intensity change at 505 nm as a function of time in a solution of berberine and (+)-fenchone after mixing with CB7 solution at 298 K. Total concentrations at t=0 s were 2.5 μM berberine, 4.9, 10.3, 18.4, 26.5, 45.4 μM (+)-fenchone (from up to down), and 0.25 μM CB7 Excitation occurred at 345 nm. The red lines represent the result of the nonlinear least-squares fit of the numerical solution of the system of differential equations. (B) Determination of the binding constant from the stopped-flow signals after reaching equilibrium.

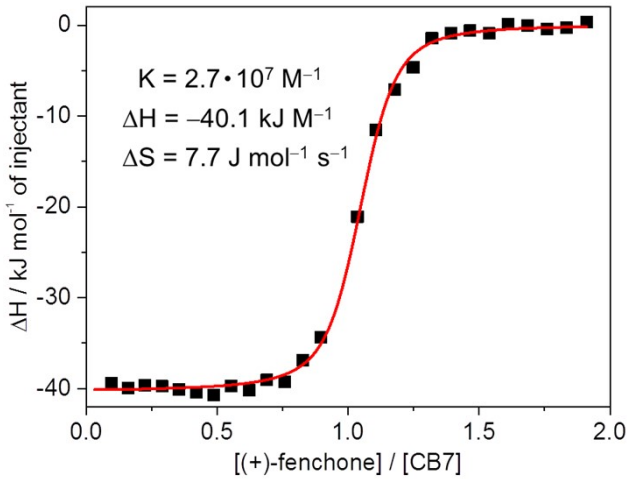

Figure S15 Integrated heat released per injection (■) for the titration of 10 μM CB7 by 100 μM (+)-fenchone solution at 298 K. The line shows the best fit with a one-site binding model.

2-adamantanone

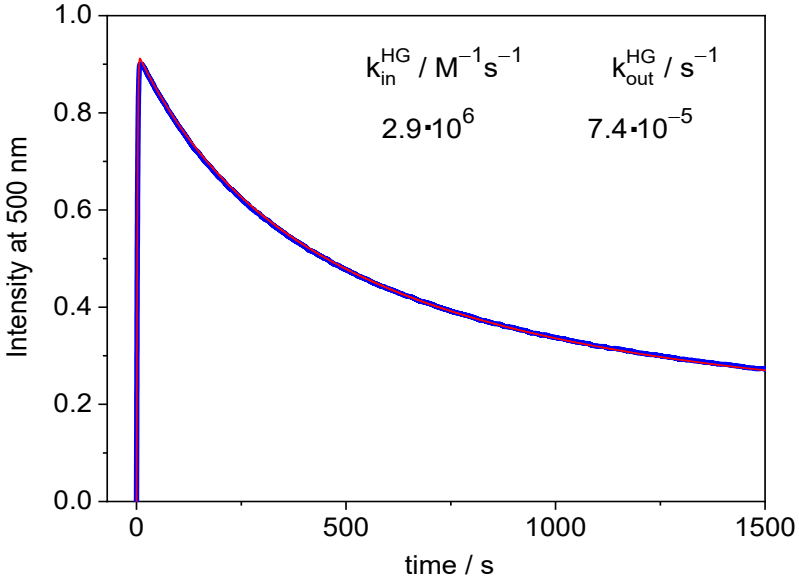

Figure S16 Fluorescence intensity change at 500 nm as a function of time in a solution of berberine and 2-adamantanone after mixing with CB7 solution at 298 K. Total concentrations at t=0 s were 15.3 μM berberine, 0.25 μM 2-adamantanone, and 0.25 μM CB7 Excitation occurred at 420 nm. The red line represents the result of the nonlinear least-squares fit of the numerical solution of the system of differential equations.

5-chloro-2-adamantanone

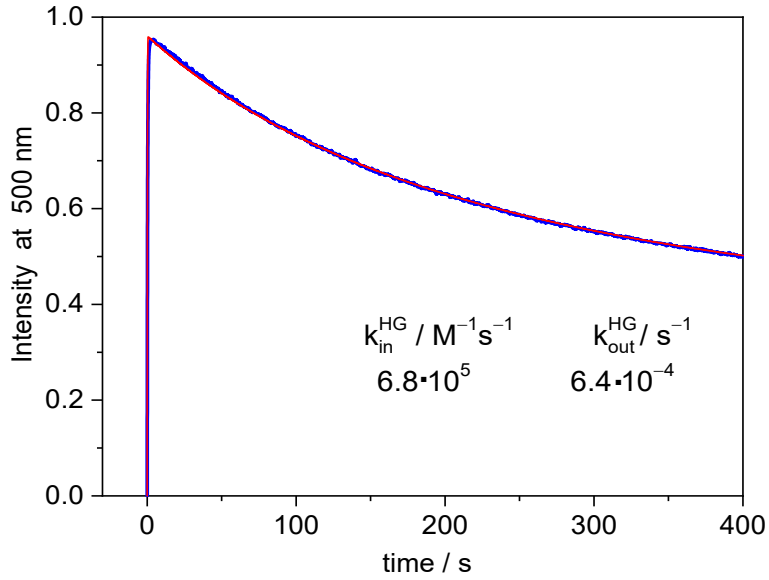

Figure S17 Fluorescence intensity change at 500 nm as a function of time in a solution of berberine and 5-chloro-2-adamantanone after mixing with CB7 solution at 298 K. Total concentrations at t=0 s were 2.5 μM berberine, 0.24 μM 5-chloro-2-adamantanone, and 0.25 μM CB7 Excitation occurred at 345 nm. The red line represents the result of the nonlinear least-squares fit of the numerical solution of the system of differential equations.

5-bromo-2-adamantanone

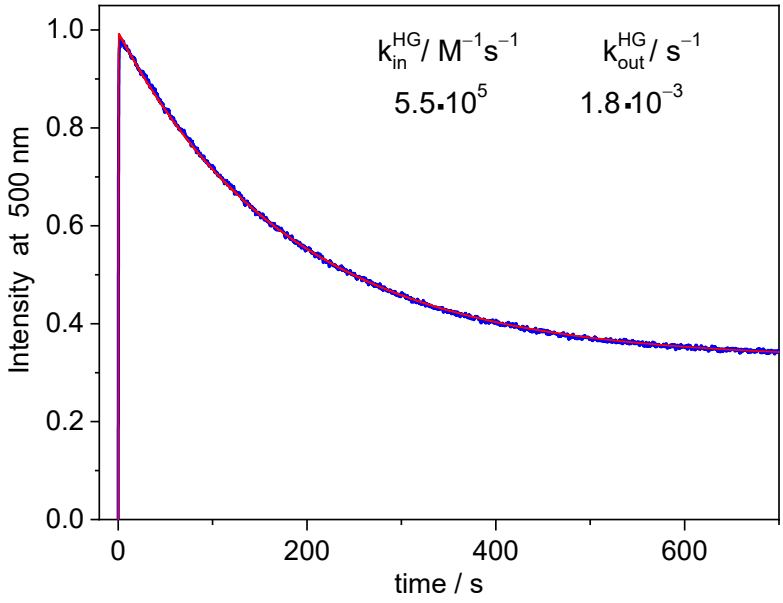

Figure S18 Fluorescence intensity change at 500 nm as a function of time in a solution of berberine and 5-bromo-2-adamantanone after mixing with CB7 solution at 298 K. Total concentrations at t=0 s were 15.5 μM berberine, 2.5 μM 5-bromo-2-adamantanone, and 0.25 μM CB7 Excitation occurred at 420 nm. The red line represents the result of the nonlinear least-squares fit of the numerical solution of the system of differential equations.

Binding to CB6

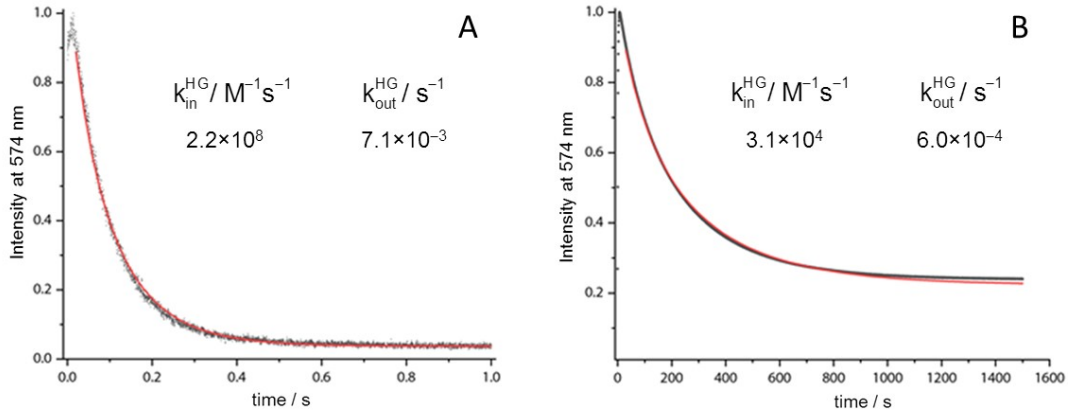

Figure S19 Fluorescence intensity variations at 574 nm as a function of time in a solution of DSMI and (A) CAD or (B) 4-MBA after mixing with CB6 solution at 298 K. Total concentrations at t=0 s were 4.0 μM DSMI, 2.0 μM CB6, 4.0 μM CAD or 4.0 μM 4-MBA. Excitation was performed at 547 nm. The red lines represent the result of the nonlinear least-squares fit of the numerical solution of the system of differential equations.

Prednisolone and nortestosterone binding in CB8 studied by N-methyl-4-pyridinylium[2.2]paracyclophane indicator

Steroids are very little soluble in aqueous solutions and tend to form aggregates like cholesterol. The aggregation of steroids precluded the study of the kinetics of their inclusion in CB8 by *kin*SBA method. DLS measurements confirmed the formation of particles.

References

1 C. D. Geddes, K. Apperson and D. J. S. Birch, *Dyes Pigments*, 2000, **44**, 69-74.

2 J. R. Dormand and P. J. Prince, *Journal of Computational and Applied Mathematics*, 1980, **6**, 19-26.

3 Z. Miskolczy, L. Biczók and G. Lendvay, *Phys. Chem. Chem. Phys.*, 2018, **20**, 15986-15994.